Solar cycle variation of ν_{max} in helioseismic data and its implications for asteroseismology

Rachel Howe [1,2]★ William J. Chaplin,[1,2]★ Sarbani Basu,[3] Warrick H. Ball [1,2] Guy R. Davies,[1,2] Yvonne Elsworth,[1,2] Steven J. Hale,[1,2] Andrea Miglio [1,2] Martin Bo Nielsen[1,2,4] and Lucas S. Viani[3]

[1]*School of Physics and Astronomy, University of Birmingham, Birmingham B15 2TT, UK*
[2]*Stellar Astrophysics Centre (SAC), Department of Physics and Astronomy, Aarhus University, Ny Munkegade 120, DK-8000 Aarhus C, Denmark*
[3]*Department of Astronomy, Yale University, P.O. Box 208101, New Haven, CT 06520-8101, USA*
[4]*Center for Space Science, NYUAD Institute, New York University Abu Dhabi, PO Box 129188, Abu Dhabi, United Arab Emirates*

ABSTRACT

The frequency, ν_{max}, at which the envelope of pulsation power peaks for solar-like oscillators is an important quantity in asteroseismology. We measure ν_{max} for the Sun using 25 yr of Sun-as-a-star Doppler velocity observations with the Birmingham Solar-Oscillations Network (BiSON), by fitting a simple model to binned power spectra of the data. We also apply the fit to Sun-as-a-star Doppler velocity data from Global Oscillation Network Group and Global Oscillations at Low Frequency, and photometry data from VIRGO/SPM on the ESA/NASA *SOHO* spacecraft. We discover a weak but nevertheless significant positive correlation of the solar ν_{max} with solar activity. The uncovered shift between low and high activity, of $\simeq 25\,\mu$Hz, translates to an uncertainty of 0.8 per cent in radius and 2.4 per cent in mass, based on direct use of asteroseismic scaling relations calibrated to the Sun. The mean ν_{max} in the different data sets is also clearly offset in frequency. Our results flag the need for caution when using ν_{max} in asteroseismology.

Key words: asteroseismology – Sun: activity – Sun: helioseismology.

1 INTRODUCTION

In the Sun and other solar-like oscillators, the frequency at which the envelope of the pulsation spectrum has its maximum in power is known as ν_{max} (Kjeldsen & Bedding 1995). The quantity plays a role in ensemble asteroseismology, as via scaling relations (e.g. Chaplin & Miglio 2013) it can be used to help constrain fundamental stellar properties, even though it is set by the characteristics of the outer layers of the star where the modes are excited and damped (Belkacem et al. 2011, 2013). Brown et al. (1991) were the first who suggested explicitly that ν_{max} might be related to the photospheric acoustic cut-off frequency, which in turn suggested a scaling with surface gravity, g, and effective temperature, T_{eff}, of the form

$$\nu_{max} \propto gT_{eff}^{-1/2} \propto M R^{-2} T_{eff}^{-1/2}, \qquad (1)$$

with M the mass and R the radius of the star. The use of ν_{max} to constrain stellar properties rests not only on the level of accuracy of this scaling (see e.g. Coelho et al. 2015; Viani et al. 2017), but also on having a robust reference to calibrate the relation. The solar ν_{max} is usually adopted as the reference. Recent estimates of it in the literature cover the range 3080–3160 µHz. This spread translates to

a difference of about 2.5 per cent in the radius and 8 per cent in the mass for a given star, based on the direct use of scaling relations (e.g. Chaplin & Miglio 2013) calibrated to the Sun.

Many estimates of the solar ν_{max} come from using photometric Sun-as-a-star data (Kallinger et al. 2010; Huber et al. 2011; Mosser, Samadi & Belkacem 2013; Kallinger et al. 2014) collected by the VIRGO/SPM instrument on the ESA/NASA *SOHO* spacecraft (Fröhlich et al. 1995). Another photometric estimate used reflected sunlight from Neptune captured by the NASA *Kepler* telescope during its extended K2 mission phase (Gaulme et al. 2016). Others have instead estimated ν_{max} using data in Doppler velocity, e.g. from the Global Oscillation Network Group (GONG) telescopes (Kiefer et al. 2018), or from the Stellar Observations Network Group spectrograph fed with scattered sunlight (Fredslund Andersen et al. 2019).

There are several factors that contribute to the spread in the reported values. Differences in methodology may play a role, e.g. the parametric model used to fit the data. For example, fits to stars and solar data typically assume a Gaussian envelope for the pulsation spectrum (e.g. Lund et al. 2017); however, the solar envelope is clearly asymmetric (Kiefer et al. 2018).

Differences related to the data are undoubtedly important, beginning with how the oscillations are observed. Doppler results tend to give a higher ν_{max} than do photometric observations.

★ E-mail: W.J.Chaplin@bham.ac.uk (WJC), R.Howe@bham.ac.uk (RH)

There are also differences between different Doppler data sets. Doppler observations are sensitive to perturbations at different heights in the stellar atmosphere, depending on the Fraunhofer line (or lines) used. The locations of the outer boundaries of the mode cavities lie beneath the photosphere, and depend on mode frequency. Perturbations due to the modes are therefore evanescent in the photosphere, with the observed signal suffering frequency-dependent attenuation with increasing height. This has the potential to affect the observed ν_{max}. Also of note is that the ratio of the amplitudes of signals due to oscillations and granulation is much lower in photometry than in Doppler velocity. This means that for photometric data, the background power spectral density is dominated in frequency by the granulation, and the oscillations are usually observed at a significantly lower signal-to-noise ratio than in Doppler velocity. Most results come from Sun-as-a-star data, which are sensitive to modes of low angular degree, *l*; but one recent estimate has been made using a much wider set of modes ($2 \leq l \leq 150$; see Kiefer et al. 2018). Finally, even though data from the same instrument may have been used, the selections are not usually contemporaneous. It is on this last point that we focus here.

While most stellar observations cover relatively short time intervals, for the Sun we have more than 20 yr of high-quality observations from multiple instruments, in multiple observables. It is therefore of interest to see how precisely we can in fact measure the solar ν_{max} over long periods of time using different instruments, as this has implications for the use of the quantity in scaling relations, and to see whether there is any intrinsic variability related to the solar cycle. That is the objective of this paper.

2 DATA AND METHODS

Our primary data set consists of Sun-as-a-star Doppler velocity observations from the Birmingham Solar-Oscillations Network (BiSON; Chaplin et al. 1996; Hale et al. 2016). The data we used cover the period 1995 to early 2018, or nearly two full solar cycles. For comparison, we also considered velocity data from the GONG (Harvey et al. 1996) and from the Global Oscillations at Low Frequency (GOLF) instrument (Gabriel et al. 1995) on *SOHO*; and photometry data from the Red channel of the VIRGO/SPM instrument (Frohlich et al. 1997), also on *SOHO*. For GONG we used the $l = 0$ spherical harmonic time series provided by the GONG project.[1] The GONG data have been treated with a first-difference filter; to correct for the effects of this on the spectral power we divide the spectrum by a factor of $4\sin^2(\pi\nu/2\nu_{Nyq})$, where ν_{Nyq} is the Nyquist frequency – 8333 μHz for the 60-s cadence of GONG. For VIRGO/SPM, we used up-to-date level-1 data[2] from the Red channel. The 22-yr GOLF data set comes from a new calibration and is an average of signals from the PM1 and PM2 detectors (Appourchaux et al. 2018).

The procedure for measuring ν_{max} over time was as follows. The time series of observations were divided into overlapping segments – each of length 1 yr, with start-time offset by 3 months – and a Fourier power spectrum was computed for each segment. Each spectrum was then averaged over a number of frequency bins of width 135 μHz, corresponding to the separation between modes of the same degree and adjacent radial order, the so-called large frequency separation $\Delta\nu$. Binning gives data that have an underlying smooth trend in frequency and statistics that tend to Gaussian.

[1] Available from gong.nso.edu
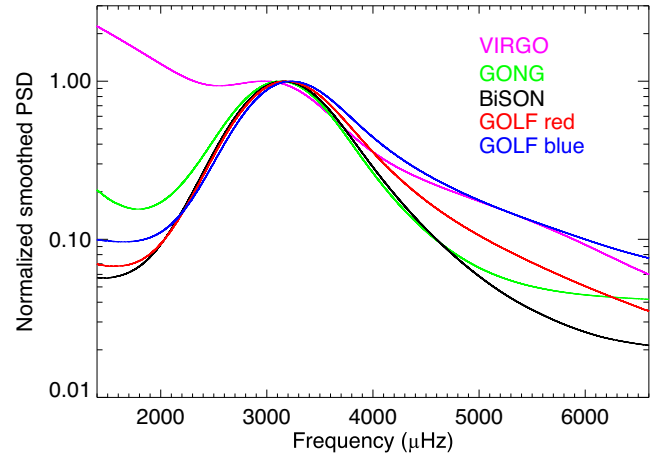[2] SOHO.nascom.nasa.gov/data/data.html

Figure 1. Mean of the bin-averaged power spectra from each full data set, normalized to show the same power spectral density at the peak of the 5-min envelope (arbitrarily scaled to unity on the ordinate).

We used the LMFIT PYTHON package (Newville et al. 2018) to perform a non-linear least-squares fit of a custom model to each binned power spectrum. Taking inspiration from Kiefer et al. (2018), the model consists of an asymmetric pseudo-Voigt profile (Stancik & Brauns 2008). There is also a frequency-dependent background term, and a constant background offset. The oscillation envelope profile takes the form

$$P(\nu) = f \times P_L(\nu) + [1-f] \times P_G(\nu), \qquad (2)$$

where ν is frequency, $P_L(\nu)$ and $P_G(\nu)$ are respectively the Lorentzian and Gaussian parts of the profile, and *f* is the factor governing the balance between the Lorentzian and Gaussian contributions. Specifically, we use

$$X = [(\nu - \nu_{max})/\Gamma(\nu)]^2, \qquad (3)$$

where

$$\Gamma(\nu) = 2\Gamma_0 / \left[1 + \exp^{[a(\nu - \nu_{max})]}\right] \qquad (4)$$

describes the frequency dependence of the width, with $\Gamma = \Gamma_0$ at $\nu = \nu_{max}$ and *a* being an asymmetry term. The Lorentzian term is

$$P_L(\nu) = \frac{2H}{(1 + 4X)\pi\Gamma(\nu)}, \qquad (5)$$

and the Gaussian term is

$$P_G(\nu) = \frac{H\sqrt{4\ln(2)}}{\pi\Gamma(\nu)\exp^{[4X\ln(2)]}}, \qquad (6)$$

where *H* governs the height of the oscillation power envelope.

A weakness of this parametrization is that if both ν_{max} and *a* are allowed to vary independently the fit results for these two parameters are highly correlated. For the final fits we therefore selected a fixed value of *a*, by repeating the fits for a range of *a* and selecting the one that gave the lowest overall χ^2 for the whole data set. For the background we tried both a Lorentzian model centred on zero frequency, and a non-parametric background given by smoothing with a median filter.

Fig. 1 shows the mean of the bin-averaged power spectra from each full data set, all normalized to show the same power spectral density at the peak of the 5-min envelope (arbitrarily scaled to unity on the plot). The figure shows clearly differences in the shape of the observed power spectra. The final fits adopted fixed values of the asymmetry parameter of $a = -0.5$ (BiSON), -0.3 (GONG), and
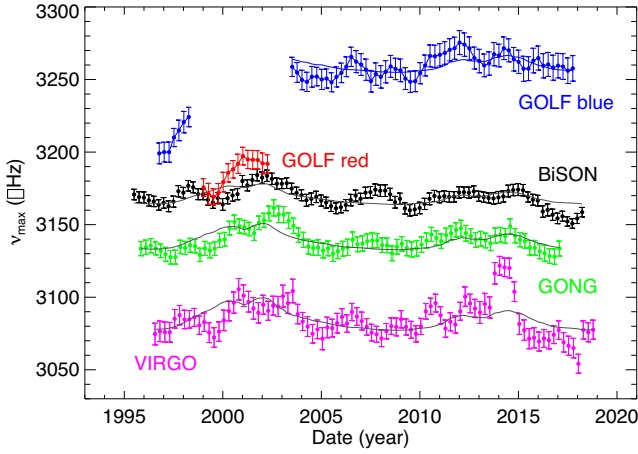
Figure 2. Best-fitting ν_{max} from each data set as a function of time (coloured points with associated error bars). The results are for BiSON (black points), GONG (green points), VIRGO (violet points), GOLF blue wing (blue points), and GOLF red wing (red points). The solid lines show the scaled 10.7 cm radio flux from fits of the linear model defined by equation (7).

−0.7 (VIRGO). Note a negative asymmetry implies more power on the high-frequency side of the oscillation envelope. Two mean spectra are shown for GOLF: one made from data collected after 1998 September and before 2002 November, when in our final fits a was fixed at −1.2; and another made from data collected at earlier and later dates, when it was fixed at $a = -1.9$. This reflected a change in the instrument's observing mode, from detecting Doppler shifts before 1998 September in the blue wing of the Sodium doublet at 589 nm; to then detecting them in the red wing up to 2002 November; and finally to detecting them back in the blue wing thereafter.
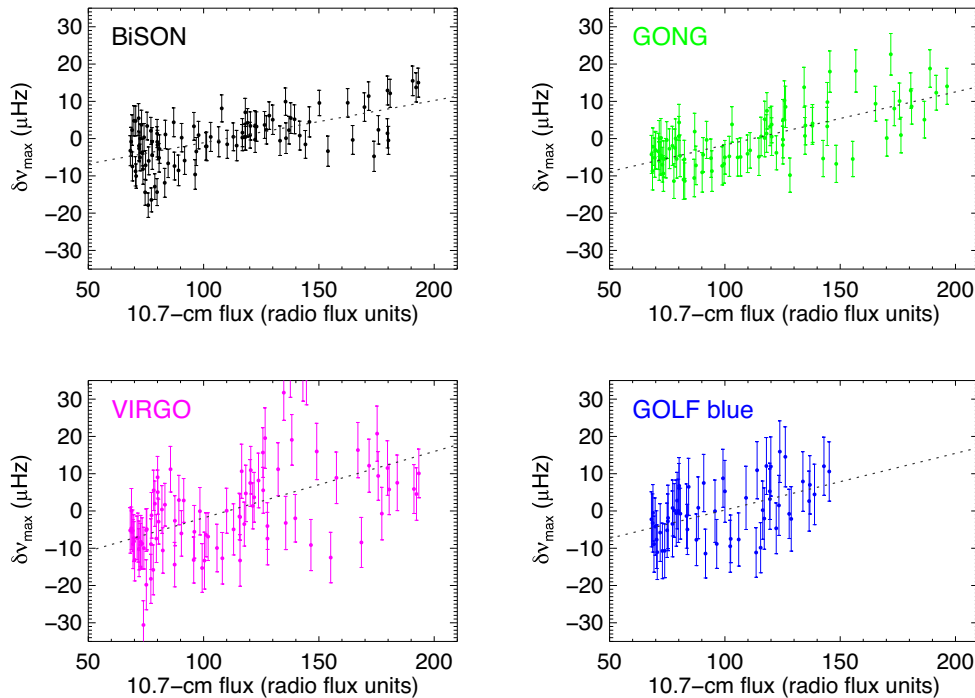
We found that the free parameter f converged on values typically around 20 per cent or lower for VIRGO, in the range 30 per cent to 40 per cent for BiSON and GONG, around 60 per cent for GOLF red wing, and even higher for GOLF blue wing.

The statistics of the bin-averaged spectrum mean that the uncertainties in each power average are highest near ν_{max}, where the modes are most prominent. That is because individual bins in each $\Delta\nu$-wide segment that contribute to the re-binned averages will span a considerable range in power, from high-power spectral densities across individual modes down to lower-power spectral densities between modes. An error-weighted fit would then be dominated by the averaged bins in the wings of the power envelope and the background, where the dispersion from individual bins contributing to each average is lower. We therefore choose to fit the logarithmic spectrum, because this gives similar relative uncertainties in every bin. We used a Monte Carlo method to estimate the uncertainties, in which the fit was repeated for 1000 realizations of each spectrum taken from a normal distribution of width $\sigma_P(\nu)$ centred on the observed value $P(\nu)$ at each frequency bin, and the uncertainty was taken to be the standard deviation of the resulting estimated parameters.

3 RESULTS

We comment first on the variability of ν_{max} over time, which is the focus of the paper. Fig. 2 shows the best-fitting ν_{max} from each data set as a function of time (coloured points with associated error bars). The results for BiSON (black points), GONG (green points), and VIRGO (violet points) show a similar pattern of variation, and a significant positive correlation with solar activity. This correlation is shown clearly in Fig. 3, which plots the best-fitting ν_{max} as a function of the 10.7 cm radio flux, $F_{10.7}$ (Tapping 2013), which we

Figure 3. Best-fitting ν_{max} as a function of the 10.7 cm radio flux, for BiSON (top left-hand panel), GONG (top right-hand panel), VIRGO (bottom left-hand panel), and GOLF blue wing (bottom right-hand panel). The dotted lines show fits of the linear model defined by equation (7).

Table 1. Results of fits of the best-fitting ν_{max} from Fig. 2 to the 10.7-cm radio flux, using the linear model described by equation (7).

| Data set	c_0 (μHz)	c_1 (μHz RF^{-1})
VIRGO	3085 ± 4	0.18 ± 0.06
GONG	3138 ± 2	0.14 ± 0.03
BiSON	3169 ± 2	0.11 ± 0.03
GOLF blue	3261 ± 4	0.15 ± 0.07

adopt as a proxy of global solar activity. The dotted lines in Fig. 3 are from fits of a simple linear model of the form:

$$\nu_{max}(t) = c_0 + c_1 \times [F_{10.7}(t) - 110].\qquad(7)$$

The offset of 110 radio flux units corresponds to the average 10.7-cm flux over the full period of the data; its introduction to the model means c_0 corresponds to ν_{max} at average activity. The solid lines in Fig. 2 show the scaled 10.7 cm radio flux from this linear model. Table 1 reports the best-fitting coefficients of each fit.

We also performed the analysis using two independent pipelines to verify the results. One pipeline (Nielsen et al. 2017) used a Markov chain Monte Carlo sampler to fit the raw (unaveraged) power spectra to a model comprising three background terms (two Lorentzians and a flat offset) and a Gaussian for the mode envelope. The other pipeline adopted a very different approach, following Huber et al. (2009). In brief, after dividing out the background – as estimated using a moving-median filter – we computed the autocorrelation of 675 μHz ($\simeq 5\Delta\nu$) wide ranges of the power spectrum, sliding a frequency window through the full spectrum. We then fitted a Gaussian to the sum over all lags to estimate ν_{max}, with the correlation between overlapping segments included in the fit. Both pipelines uncovered the same temporal variations as our main pipeline, showing our results on the time variation of ν_{max} are robust against the choice of fitting model and fitting procedure.

We see a positive shift in ν_{max} of $\simeq 25\,\mu$Hz between low and high activity. The results for GOLF are however more complicated, and are dominated by the change in observing mode. ν_{max} is around 80 μHz lower in the red-wing data than it is in the blue-wing data. If we separate out the blue-wing data, which cover a much longer period, it too shows a positive correlation with activity.
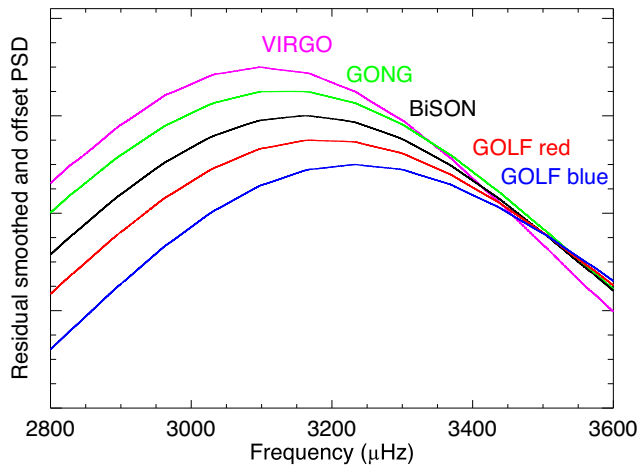
Barban et al. (2013) studied the solar ν_{max} in data from GOLF and VIRGO collected between 1996 and 2004 and found that the GOLF ν_{max} appeared to be anticorrelated with the sunspot number but that from VIRGO was not. Based on our results above, it now seems clear that the apparent anticorrelation with activity they reported is actually due to the change in operation from one wing to another (and back again). That Barban et al. (2013) found no apparent change in the VIRGO ν_{max} is likely due to them having had less data than are available to us now, i.e. the changes we uncover, whilst significant, are none the less quite weak.

Our results also show significant differences in the average ν_{max} for the different data sets (e.g. see the c_0 estimates in Table 1). The left-hand panel of Fig. 4 shows a zoom of the mean spectra from Fig. 1 *after* a mean best-fitting background model was removed from each. The residual spectra have then been offset on the ordinate to show more clearly the differences in ν_{max}. The absolute spread is noticeably larger than the activity-related variations. The photometric VIRGO results show the lowest average ν_{max}. The right-hand panel shows a zoom of mean BiSON spectra from epochs of low and high activity (centred on epochs around 2001 and 2017, respectively). The cycle-related shift is clearly visible.

4 DISCUSSION AND CONCLUSIONS

We have discovered a weak but nevertheless significant positive correlation of the solar ν_{max} with solar activity. The uncovered shift, of $\simeq 25\,\mu$Hz between low and high activity, translates to an uncertainty of up to 0.8 per cent in radius and 2.4 per cent in mass, based on using the Sun as a calibrator in direct use of the scaling relations. Our result also suggests that we might expect to find variations of ν_{max} in other stars, which would add additional uncertainty to any inferences made using this global asteroseismic parameter (a point we come back to below).

The underlying causes of the variations we have uncovered in the solar ν_{max} must be intimately tied to variations in the power and damping of the modes. There is an extensive literature (see Howe et al. 2015, and references therein) showing that p-mode powers decrease whilst damping rates increase as levels of solar activity rise. The interplay between the relative sizes of these changes with frequency will determine the variation of ν_{max}.
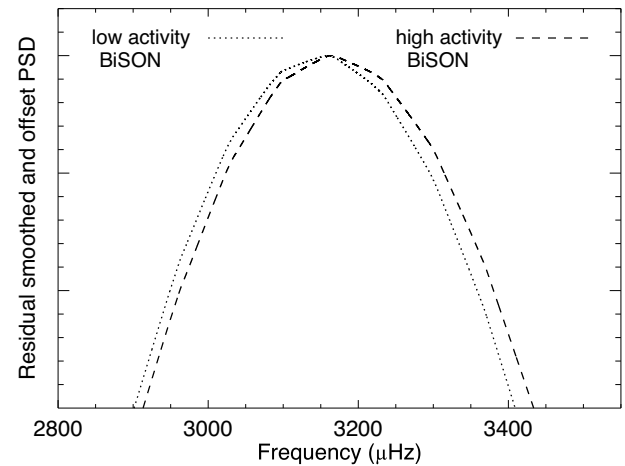
Figure 4. Left-hand panel: Zoom of the mean spectra from Fig. 1 after a best-fitting background model was removed from each spectrum. The residual spectra have then been offset on the ordinate. Right-hand panel: zoom of mean BiSON spectra from epochs of low and high activity (centred on epochs around 2001 and 2017, respectively).

As noted earlier, the scaling relation for ν_{max} arose by assuming a proportionate scaling with the photospheric acoustic cut-off frequency. It is therefore intriguing to note that Jiménez, García & Pallé (2011) found a clear positive correlation of the solar cut-off frequency with solar activity. The fractional change they found is about four times larger than the fractional change we have uncovered in ν_{max}.

We also find significant differences in the average ν_{max} given by the various data sets. The ordering of ν_{max} does not respect a simple correlation (or anticorrelation) with the average height above the base of the photosphere at which the observations are effectively made. A correlation with increasing atmospheric height would, moving outwards, suggest (e.g. see Jiménez-Reyes et al. 2007) an ordering in ν_{max} of VIRGO/SPM, GONG, BiSON, GOLF blue, and finally GOLF red (and a reversed order for an anticorrelation); this is not quite what we see. Nevertheless, that there is such a dramatic change between GOLF red and GOLF blue shows that the way the observations are made matters (see also García et al. 2005). Understanding these absolute differences more clearly will be the focus of future work.

Our results clearly flag the need for caution when using ν_{max} on other stars. They sound a warning over making sure one has a solar reference extracted from data with the same instrumental response as the stellar data, using the same analysis methodology, and for a clearly defined level of solar activity. Since changing levels of activity perturb the solar ν_{max}, a desirable reference would be one commensurate with minimal levels of activity (corresponding to minimal impact on ν_{max}). But the stellar ν_{max} must then also be compatible with regard to activity levels, which may not always be possible to achieve.

REFERENCES

Appourchaux T., Boumier P., Leibacher J. W., Corbard T., 2018, A&A, 617, A108
Astropy Collaboration, 2013, A&A, 558, A33
Barban C., Beuret M., Baudin F., Belkacem K., Goupil M. J., Samadi R., 2013, J. Phys. Conf. Ser., 440, 012031
Belkacem K., Goupil M. J., Dupret M. A., Samadi R., Baudin F., Noels A., Mosser B., 2011, A&A, 530, A142
Belkacem K., Samadi R., Mosser B., Goupil M. J., Ludwig H. G., 2013, in Shibahashi H., Lynas-Gray A. E., eds, ASP Conf. Ser. Vol. 479, Progress in Physics of the Sun and Stars: A New Era in Helio- and Asteroseismology. Astron. Soc. Pac., San Francisco, p. 61
Brown T. M., Gilliland R. L., Noyes R. W., Ramsey L. W., 1991, ApJ, 368, 599
Chaplin W. J., Miglio A., 2013, ARA&A, 51, 353
Chaplin W. J. et al., 1996, Sol. Phys., 168, 1
Coelho H. R., Chaplin W. J., Basu S., Serenelli A., Miglio A., Reese D. R., 2015, MNRAS, 451, 3011
Fredslund Andersen M. et al., 2019, A&A, 623, L9
Fröhlich C. et al., 1995, Sol. Phys., 162, 101
Frohlich C. et al., 1997, Sol. Phys., 170, 1
Gabriel A. H. et al., 1995, Sol. Phys., 162, 61
García R. A. et al., 2005, A&A, 442, 385
Gaulme P. et al., 2016, ApJ, 833, L13
Hale S. J., Howe R., Chaplin W. J., Davies G. R., Elsworth Y. P., 2016, Sol. Phys., 291, 1
Harvey J. W. et al., 1996, Science, 272, 1284
Howe R., Davies G. R., Chaplin W. J., Elsworth Y. P., Hale S. J., 2015, MNRAS, 454, 4120
Huber D., Stello D., Bedding T. R., Chaplin W. J., Arentoft T., Quirion P. O., Kjeldsen H., 2009, Commun. Asteroseismol., 160, 74
Huber D. et al., 2011, ApJ, 743, 143
Jiménez A., García R. A., Pallé P. L., 2011, ApJ, 743, 99
Jiménez-Reyes S. J., Chaplin W. J., Elsworth Y., García R. A., Howe R., Socas-Navarro H., Toutain T., 2007, ApJ, 654, 1135
Jones E. et al., 2001, SciPy: Open Source Scientific Tools for Python, http://www.scipy.org/
Kallinger T. et al., 2010, A&A, 522, A1
Kallinger T. et al., 2014, A&A, 570, A41
Kiefer R., Komm R., Hill F., Broomhall A.-M., Roth M., 2018, Sol. Phys., 293, 151
Kjeldsen H., Bedding T. R., 1995, A&A, 293, 87
Lund M. N. et al., 2017, ApJ, 835, 172
Mosser B., Samadi R., Belkacem K., 2013, in Cambresy L., Martins F., Nuss E., Palacios A., eds, SF2A-2013: Proceedings of the Annual Meeting of the French Society of Astronomy and Astrophysics. SF2A, France, p. 25
Newville M. et al., 2018, lmfit-py 0.9.12
Nielsen M. B., Schunker H., Gizon L., Schou J., Ball W. H., 2017, A&A, 603, A6
Oliphant T. E., 2006, A Guide to NumPy. Createspace Independent Publishing Platform
Price-Whelan A. M. et al., 2018, AJ, 156, 123
Stancik A. L., Brauns E. B., 2008, Vib. Spectrosc., 47, 66
Tapping K. F., 2013, Space Weather, 11, 394
Viani L. S., Basu S., Chaplin W. J., Davies G. R., Elsworth Y., 2017, ApJ, 843, 11

[3] http://www.astropy.org

This paper has been typeset from a TEX/LATEX file prepared by the author.